Creation of radially polarized optical fields with multiple controllable parameters using a vectorial optical field generator

Sichao Zhou,[1] Shiyi Wang,[2] Jian Chen,[1,3] Guanghao Rui,[4] and Qiwen Zhan[1,*]

[1]*Electro-Optics Graduate Program, University of Dayton, 300 College Park, Dayton, Ohio 45469-2951, USA*
[2]*Globalfoundries, 2070 Route 52, Hopewell Junction, New York 12533, USA*
[3]*School of Electronic Engineering, University of Electronic Science and Technology of China, Chengdu 610054, China*
[4]*Advanced Photonics Center, Southeast University, Nanjing 210096, China*
**Corresponding author: qzhan1@udayton.edu*

Received April 28, 2016; accepted August 24, 2016;
posted September 1, 2016 (Doc. ID 264212); published September 23, 2016

A vectorial optical field generator (VOF-Gen) based on two reflective phase-only liquid crystal spatial light modulators enables the creation of an arbitrary optical complex field. In this work, the capabilities of the VOF-Gen in terms of manipulating the spatial distributions of phase, amplitude, and polarization are experimentally demonstrated by generating a radially polarized optical field consisted of five annular rings, the focusing properties of which are also numerically studied with vectorial diffraction theory. By carefully adjusting the relative amplitude and phase between the adjacent rings, an optical needle field with purely longitudinal polarization can be produced in the focal region of a high numerical aperture lens. The versatile method presented in this work can be easily extended to the generation of a vectorial optical field with any desired complex distributions.

OCIS codes: (260.5430) Polarization; (070.6120) Spatial light modulators; (140.3300) Laser beam shaping; (050.1970) Diffractive optics.
http://dx.doi.org/10.1364/PRJ.4.000B35

1. INTRODUCTION

In the last decade, the longitudinally polarized optical needle field (ONF) with a long depth of focus (DOF) has drawn a significant amount of attention due to its fascinating properties and potential applications [1], for examples, in optical trapping and manipulation [2,3], particle acceleration [4,5], optical data storage [6], and biomedical imaging [7,8]. Such an ONF can be realized through tight focusing of a radially polarized light passing through a multibelt binary pupil filter [9–12]. However, all these methods suffer from the energy loss of pupil filters, and each specific vector beam requires an individual filter design, which fails to manipulate light dynamically, leading to high cost and limited efficiency for practical applications. On the other hand, various approaches have been proposed to enhance or suppress the longitudinal field component, including through modulating the amplitude, polarization, and phase of the incident light [13–15]. Hence, generation of controllable spatially variant vectorial optical fields on the incident plane without any pupil filters is very attractive to achieve a high purity ultralong ONF.

Owing to their unique properties, optical fields with spatially inhomogeneous state of polarization (SOP) or other complex phase and amplitude distribution in the beam cross section have attracted increasing interest. For example, the orbital angular momentum carried by a vortex beam enables a considerable increase in the capacity of the network [16], radially polarized beam can boost the efficiency of a plasmonic lens [17], high order full Poincaré beams can be utilized to generate a flattop distribution [18], and so on. In the past few years, several methods have been proposed to modulate the optical field with a metasurface [19–21]. However, these subwavelength metallic components suffer from low efficiency and a complicated fabrication process. Besides, the functionalities of the metasurface are strongly determined by both the geometry and material of the micro–nano unit design, leading to the difficulty in dynamically modulating the optical field. Recently, several methods have been demonstrated to develop versatile systems for the generation of arbitrary optical vector fields with single spatial light modulators (SLMs) [22–24]. However, due to the limitation of single SLMs, it still remains a great challenge to control the amplitude, phase, and polarization of optical beams independently. As a result, the generation of an arbitrary vectorial optical field cannot be fully realized with those techniques. It is noteworthy that all these techniques are unable to create a spatially invariant arbitrary vectorial optical field with high spatial resolution on a pixel basis in the incident plane for ONF generation.

Recently, a vectorial optical field generator (VOF-Gen) that is capable of creating an arbitrary optical field with independent controls of phase, amplitude, and polarization distribution on the pixel level based on two high-resolution reflective phase-only liquid crystal (LC) SLMs has been proposed and demonstrated [25]. In this paper, we generate a radially polarized optical field with complex amplitude and phase distributions using the VOF-Gen. The powerful capabilities of the VOF-Gen provide an alternative way to create the desired vectorial optical field required for ONF

without the use of pupil filters. Numerical simulation results show that a DOF as long as 5λ and longitudinal polarization with high purity ONF can be obtained by tightly focusing such a radially polarized optical complex field.

2. EXPERIMENTAL SETUP

The diagram of the experimental setup for generation of arbitrary spatially variant vectorial optical field is illustrated in Fig. 1(a), which is based on two reflective phase only LC-SLMs (HOLOEYE 1080P) [25]. In order to control the four degrees of freedom of an optical field (including phase, amplitude, polarization, and retardation) with high efficiency and compact layout, each SLM panel is divided into two sections with the same area. Each section of the SLM panels is responsible to control one degree of freedom of the optical fields to be generated.

A collimated and expanded linearly polarized HeNe laser (632.8 nm) is used as the light source. The combination of a half-wave plate (HWP) and polarizer P1 is used to adjust the intensity and polarization direction of the incident beam. Spatial filters SF1 and SF2 placed in the Fourier planes of the 4-f systems are used to eliminate the high spatial frequency components as shown in Fig. 1(a). In order to realize amplitude modulation and polarization rotation, a key component called a polarization rotator (PR) is used in the VOF-Gen system, which is illustrated in Fig. 1(b). The detail of the PR setup and the modulation of each individual degree of freedom describing an optical field can be found in [24]. The Jones vector for the resulting output field is given as follows:

$$J_{\mathrm{SLM4}}(x,y) = A_0(x,y)\,\sin\left(\frac{\delta_2(x,y)}{2}\right)e^{i\left(\frac{\delta_2(x,y)}{2}+\frac{\delta_3(x,y)}{2}+\pi\right)} \times \begin{pmatrix} \cos\left(\frac{\delta_3(x,y)}{2}+\frac{\pi}{2}\right)e^{i\delta_4(x,y)} \\ \sin\left(\frac{\delta_3(x,y)}{2}+\frac{\pi}{2}\right) \end{pmatrix}, \tag{1}$$

where $A_0(x,y)$ is the amplitude for the incident beam, and $\delta_1(x,y)$, $\delta_2(x,y)$, $\delta_3(x,y)$, and $\delta_4(x,y)$ are the phases loaded to corresponding SLM sections. Through doing so, the phase, amplitude, and polarization distribution of optical fields can be modulated by programming the two high resolution reflective phase-only LC-SLMs, and all the degrees of freedoms of an optical field can be modulated independently and simultaneously with the VOF-Gen system.

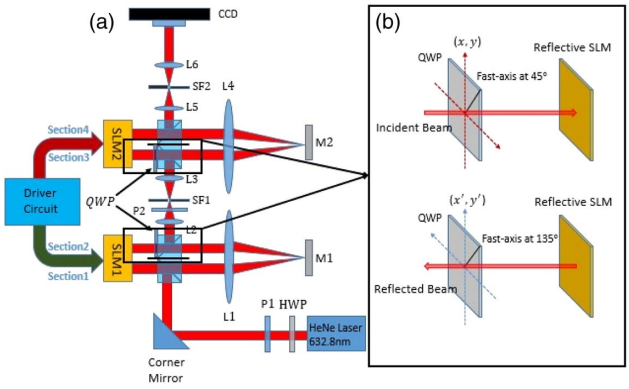

Fig. 1. VOF-Gen. (a) Schematic diagram of experimental setup. P, polarizer; L, lens; M, mirror; QWP, quarter-wave plate; SF, spatial filter. (b) Illustration of the PR setup and the effective rotation of the QWP fast axis for the incident (upper) and the reflected (lower) beams due to the mirror imaging of the laboratory coordinates in dashed lines.

3. RESULTS AND DISCUSSION

It is known that tightly focused radial polarization leads to a strong longitudinal electric field. In order to generate an ultralong ONF, both the spatial distribution of the amplitude and the phase of a radially polarized light are necessary to be adjusted. A five ring structured vectorial optical field in the pupil plane is designed by the method based on reversing the radiation of an electric dipole array, giving rise to an ONF with DOF of 5λ after focusing by a high numerical aperture (NA) objective lens [10]. With the VOF-Gen system, the desired radially polarized vectorial optical field with spatially variant phase and amplitude distributions is experimentally generated and tested. We also explore the potential to produce a high purity longitudinal polarized ONF by the experimentally generated optical pattern.

The structure and parameters of the required optical field along the radius at the pupil plane are shown in Fig. 2, where five annular rings with discrete normalized amplitude are marked with corresponding numbers according to [10,20]. The amplitude of the region between bright rings and the innermost core zone is set to zero, while the other bright rings will have their corresponding amplitudes that can be realized by loading appropriate phase information on SLM section 2. Each ring takes binary phase values that alternate between 0 and π from one ring to the next. Moreover, the desired optical field at the pupil plane is designed to be radially polarized. Thus, polarization retardation modulation is not necessary in this case. Due to the alternating phase, the polarization actually flips its directions between adjacent rings. The corresponding phase patterns loaded on VOF-Gen for such a radially polarized field are displayed in Fig. 3.

The overall phase pattern for the desired optical pattern shown in Fig. 3 is composed of two color gray-scale images, red and green. The grey level is from 0 to 255, and each of the grey levels map one actual phase value generated by the SLM. For any phase value to be generated by the SLM, a grey level is found by interpolating the phase value from an experimentally determined nonlinear calibration curve. As previously mentioned, in order to generate optical fields with arbitrarily structured phase, amplitude, and SOP, the VOF-Gen requires four

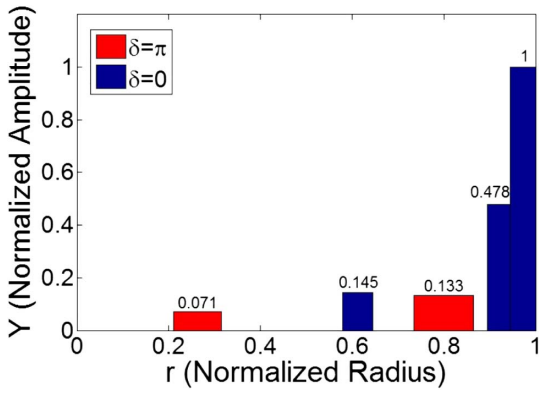

Fig. 2. Structure and parameters of the desired optical field.

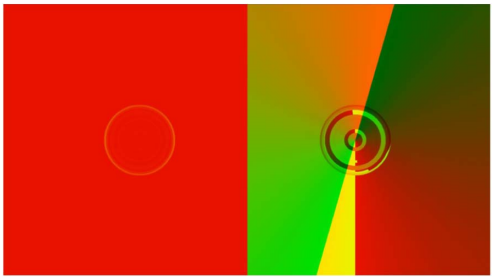

Fig. 3. Overall phase patterns displayed on VOF-Gen.

SLM sections divided from two SLM panels. SLM 1 only reads the green color information, and SLM 2 only reads the red information from the overall phase pattern image shown in Fig. 3. Consequently, the left half-window for this phase pattern image provides the required phase for amplitude and polarization retardation modulations (SLM sections 2 and 4), and the phase information of the right half-window will control phase and polarization rotation modulations (SLM sections 1 and 3). Therefore, all the characters of the desired optical pattern could be manipulated by the SLMs after loading such a phase pattern. The theoretical and experimental intensity distributions of the desired optical field in the pupil plane are shown in Figs. 4(a) and 3(b), respectively.

Note that the entire SLM window was illuminated by a collimated Gaussian beam before the amplitude modulation. The Gaussian profile of the illumination is measured and considered in order to realize the desired final amplitude distribution. The comparison of experimental and theoretical results of amplitude modulation is shown in Fig. 4(c). From the comparison, the amplitude modulation for rings 4, 5 obtained by the CCD camera matches very well with the theoretical design. However, the amplitude modulations for the first three rings are still a little higher than the theoretical results. This discrepancy is mainly introduced by background leakage between those rings that has not been entirely removed. This is due to the fact that reduction of the pinhole size in the Fourier plane of the 4-f system will eliminate both the leakage and high frequency components. In order to maintain a high resolution, we need to balance the pinhole size such that high frequency terms are well preserved while only allowing a minimum amount of leakage.

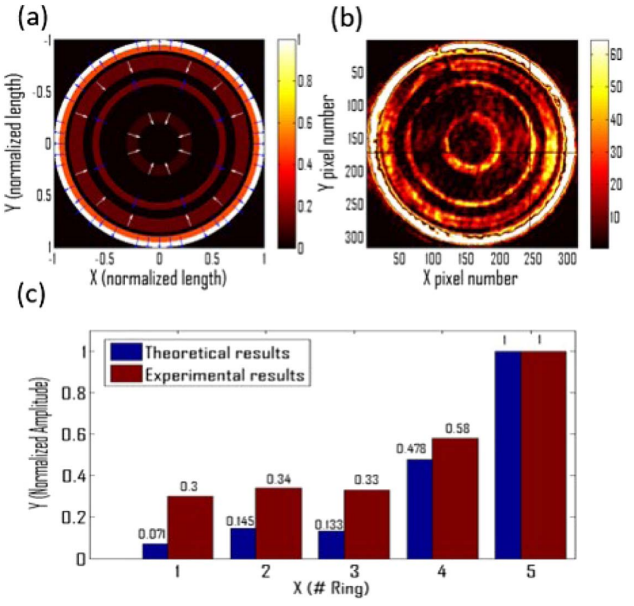

Fig. 4. Intensity distribution for desired optical field in the pupil plane: (a) theoretical and (b) experimental results. (c) Averaged amplitude distribution for experimental and theoretical results.

The theoretical and experimental intensity distributions for the desired optical fields after a linear polarizer at 0°, 45°, 90°, and 135° are shown in Fig. 5. As shown in the figure, radial polarization in the output field is observed and the spatially variant polarization rotation capability is demonstrated.

To demonstrate the capability of phase modulation, also showing the π phase jump between adjacent rings for the desired pattern, we design a simple phase pattern loaded on SLM section 1 with one half-coded with π phase and the other with zero phase. SLM section 2 is loaded with a flat phase pattern for 100% transmission, and SLM sections 3 and 4 both have zero phase. The required phase pattern is displayed in Fig. 6(b). An interference setup [Fig. 6(a)] consisting of a beamsplitter and two mirrors is used to verify the π phase shift. The input beam after the full modulation by VOF-Gen directly goes through the beamsplitter and is collected by the CCD camera. The reference beam carrying the same phase information as the input beam will be reflected by two mirrors and eventually into the CCD. As shown in Fig. 6(c), interference fringes located in the left part and right part were complementary, which means the π phase difference between the left and right parts of the pattern has been proved.

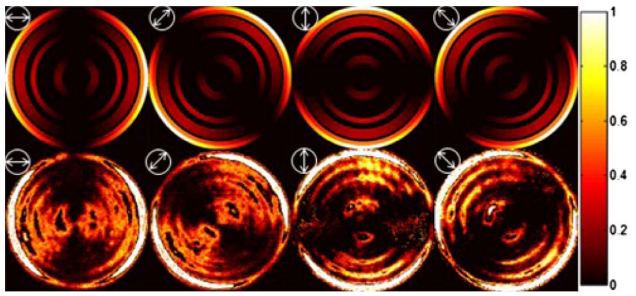

Fig. 5. Intensity distribution for five ring structured radially polarized fields after a polarizer with transmission axis orientation indicated by the arrows at 0°, 45°, 90°, and 135°. The upper row shows the theoretical results, and the lower row is for the experimental results.

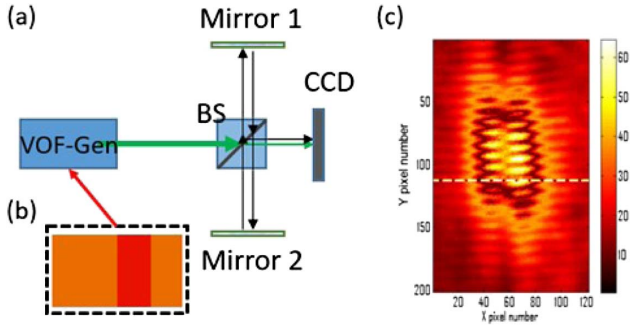

Fig. 6. (a) Interference setup to verify the π phase shift that consists of a beamsplitter (BS) and two mirrors. (b) The required phase pattern loaded on VOF-Gen for π shift verification. (c) Interference fringes patterns of π phase jump.

At this point, the capability of modulating phase, amplitude, and polarization rotation to generate desired optical fields has been successfully demonstrated. Such a method provides a convenient and dynamic way to generate spatially variant vectorial optical fields at the incident plane for ONF generation.

In order to create a needle-like field with high purity longitudinal polarization and uniform axial intensity, it is important to tailor the phase or amplitude distribution of the incident radially polarized beam. Therefore, in practical application, the deviation of the size, phase, and amplitude distribution in each ring will influence the quality of ONF generation. To explore the focusing properties of such a radial-variant vector field and how the deviation of the amplitude distribution from the theoretically designed values affects the ONF generation, we numerically calculate the total intensity pattern and the electric field distribution within the focal volume with the measured parameters. Because the structure and phase modulation of our result pattern agree with the theoretical design very well, we only study the effects arising from the amplitude deviation. The numerically calculated focal fields are illustrated in Fig. 7.

The parameters of the outermost region (rings 4 and 5) strongly influence the longitudinal components in the focal region while the uniformity in the axial intensity distribution of the focal field and the DOF mainly depend on the characteristics of the inner zone (the first three rings) [10]. The numerical simulation results based on the experimentally obtained amplitude values are shown in Figs. 7(b) and 7(d), respectively. The outermost annular zone has the largest incident angle and the highest field amplitude; thus the quality of the ONF should be most sensitive to imperfections of this zone. The simulation results demonstrate that the electric field distribution calculated with the experimentally obtained amplitude values still kept the optical needle structure, owing to the good agreement of the amplitude modulation for the outermost zone with the theoretical design. However, comparing the results shown in Figs. 7(b) and 7(d) with the theoretical results in Figs. 7(a) and 7(c), one can find a saddle region with a 40% drop in intensity near the focus along the axial direction. This is mainly attributed to the deviation of the experimentally generated amplitude values from the theoretically calculated amplitudes for the inner rings.

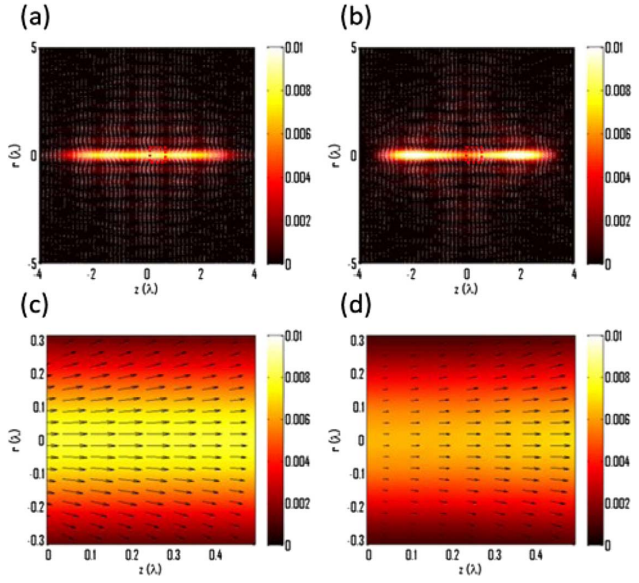

Fig. 7. Intensity distributions and the electric field distributions in the focal region of a high NA (NA = 0.95) objective lens (the polarization direction for the ONF is represented by arrows). (a) ONF calculated with the theoretical amplitude values; (b) focal field calculated with the experimentally obtained amplitude values; (c) zoomed-in picture of the area enclosed within the red dashed box in (a); (d) zoomed-in picture of the area enclosed within the red dashed box in (b).

4. CONCLUSIONS

In summary, we have demonstrated a dynamic and reliable method for engineering the radial-variant polarization field with multiple parameters. The capability to generate spatially variant phase, amplitude, and polarization rotation has been verified. As one example, an engineered optical field that could be directly focused by a high NA lens to produce a longitudinally polarized ONF without any pupil filter is demonstrated. Our scheme can be extended to dynamically generate other types of vectorial fields with desirable parameters that pave the way for their applications in many areas such as high-resolution imaging, optical tweezers, and beam shaping.

REFERENCES

1. Q. Zhan, "Cylindrical vector beams: from mathematical concepts to applications," Adv. Opt. Photon. **1**, 1–57 (2009).
2. O. M. Maragò, P. H. Jones, P. G. Gucciardi, G. Volpe, and A. C. Ferrari, "Optical trapping and manipulation of nanostructures," Nat. Nanotechnol. **8**, 807–819 (2013).
3. Q. Zhan, "Trapping metallic Rayleigh particles with radial polarization," Opt. Express **12**, 3377–3382 (2004).
4. J. R. Fontana and R. H. Pantell, "A high-energy, laser accelerator for electrons using the inverse Cherenkov effect," J. Appl. Phys. **54**, 4285–4288 (1983).
5. R. D. Romea and W. D. Kimura, "Modeling of inverse Čerenkov laser acceleration with axicon laser-beam focusing," Phys. Rev. D **42**, 1807–1818 (1990).
6. Y. Zhang and J. Bai, "Improving the recording ability of a near-field optical storage system by higher-order radially polarized beams," Opt. Express **17**, 3698–3706 (2009).
7. L. Novotny, M. R. Beversluis, K. S. Youngworth, and T. G. Brown, "Longitudinal field modes probed by single molecules," Phys. Rev. Lett. **86**, 5251–5254 (2001).
8. T. A. Planchon, L. Gao, D. E. Milkie, M. W. Davidson, J. A. Galbraith, C. G. Galbraith, and E. Betzig, "Rapid three-dimensional isotropic imaging of living cells using Bessel beam plane illumination," Nat. Methods **8**, 417–423 (2011).
9. H. Wang, L. Shi, B. Lukyanchuk, C. Sheppard, and C. T. Chong, "Creation of a needle of longitudinally polarized light in vacuum using binary optics," Nat. Photonics **2**, 501–505 (2008).
10. J. Wang, W. Chen, and Q. Zhan, "Engineering of high purity ultralong optical needle field through reversing the electric dipole array radiation," Opt. Express **18**, 21965–21972 (2010).
11. H. Dehez, A. April, and M. Piché, "Needles of longitudinally polarized light: guidelines for minimum spot size and tunable axial extent," Opt. Express **20**, 14891–14905 (2012).
12. H. Guo, X. Weng, M. Jiang, Y. Zhao, G. Sui, Q. Hu, Y. Wang, and S. Zhuang, "Tight focusing of a higher-order radially polarized beam transmitting through multi-zone binary phase pupil filters," Opt. Express **21**, 5363–5372 (2013).
13. R. Dorn, S. Qubis, and G. Leuchs, "Sharper focus for a radially polarized light beam," Phys. Rev. Lett. **91**, 233901 (2003).
14. C. J. R. Sheppard and A. Choudhury, "Annular pupils, radial polarization, and superresolution," Appl. Opt. **43**, 4322–4327 (2004).
15. R. Fontana and R. H. Pantell, "A high-energy laser accelerator for electrons using the inverse Cerenkov effect," J. Appl. Phys. **54**, 4285–4288 (1983).

16. G. Gibson, J. Courtial, M. Padgett, M. Vasnetsov, V. Pas'ko, S. Barnett, and S. Franke-Arnold, "Free-space information transfer using light beams carrying orbital angular momentum," Opt. Express **12**, 5448–5456 (2004).
17. W. Chen, D. C. Abeysinghe, R. L. Nelson, and Q. Zhan, "Plasmonic lens made of multiple concentric metallic rings under radially polarized illumination," Nano Lett. **9**, 4320–4325 (2009).
18. W. Han, W. Cheng, and Q. Zhan, "Flattop focusing with full Poincaré beams under low numerical aperture illumination," Opt. Lett. **36**, 1605–1607 (2011).
19. N. Yu, P. Genevet, M. A. Kats, F. Aieta, J. P. Tetienne, F. Capasso, and Z. Gaburro, "Light propagation with phase discontinuities: generalized laws of reflection and refraction," Science **334**, 333–337 (2011).
20. S. Wang and Q. Zhan, "Reflection type metasurface designed for high efficiency vectorial field generation," Sci. Rep. **6**, 29626 (2016).
21. J. Lin, P. Genevet, M. A. Kats, N. Antoniou, and F. Capasso, "Nanostructured holograms for broadband manipulation of vector beams," Nano Lett. **13**, 4269–4274 (2013).
22. Z. Chen, T. Zeng, B. Qian, and J. Ding, "Complete shaping of optical vector beams," Opt. Express **23**, 17701–17710 (2015).
23. S. Tripathi and K. C. Toussaint, Jr., "Versatile generation of optical vector fields and vector beams using a noninterferometric approach," Opt. Express **20**, 10788–10795 (2012).
24. I. Moreno, J. A. Davis, T. M. Hernandez, D. M. Cottrell, and D. Sand, "Complete polarization control of light from a liquid crystal spatial light modulator," Opt. Express **20**, 364–376 (2012).
25. W. Han, Y. Yang, W. Cheng, and Q. Zhan, "Vectorial optical field generator for the creation of arbitrarily complex fields," Opt. Express **21**, 20692–20706 (2013).